Supporting Information

Engineered high-affinity dual targeting cellular nanovesicles for optimized cancer immunotherapy

Luyao Zhang [1, †], Xu Zhao [2, †], Yanan Niu [2], Xiaoya Ma [2], Wei Yuan [2, *], Jie Ma [1, *]

[1] *Center of Biotherapy, Beijing Hospital, National Center of Gerontology, Institute of Geriatric Medicine Chinese Academy of Medical Sciences, Beijing, 100730, P.R. China.*

[2] *State Key Laboratory of Molecular Oncology, National Cancer Center/National Clinical Research Center for Cancer/Cancer Hospital, Chinese Academy of Medical Sciences and Peking Union Medical College, Beijing, 100021, P.R. China.*

[†] *These authors contributed equally to this work.*

[*] *Corresponding authors.*

E-mail: majie4685@bjhmoh.cn, majie@cicams.ac.cn (Jie Ma);

yuanwei@cicams.ac.cn (Wei Yuan)

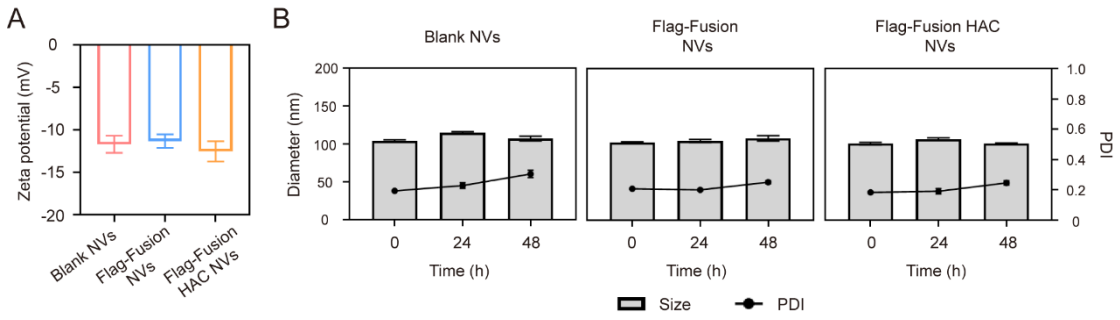

Figure S1. A) The surface ζ potential of Blank, Flag-Fusion, and Flag-Fusion HAC NVs. **B)** The size distribution and polydispersion index (PDI) changes of Blank, Flag-Fusion, and Flag-Fusion HAC NVs in physiological solution at 4℃ within 48h.

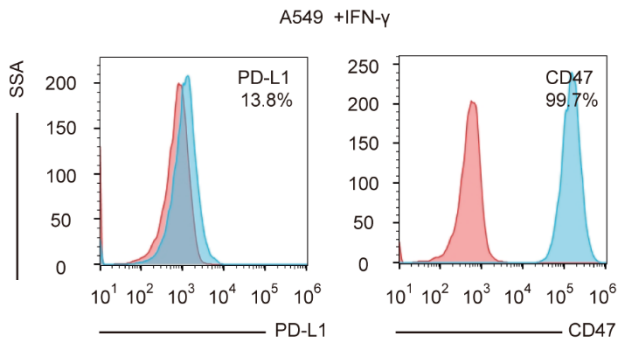

Figure S2. The expression level of PD-L1 and CD47 was measured by flow cytometry in A549 (Red: Isotype antibody; Blue: anti-PD-L1, or anti-CD47 antibody).

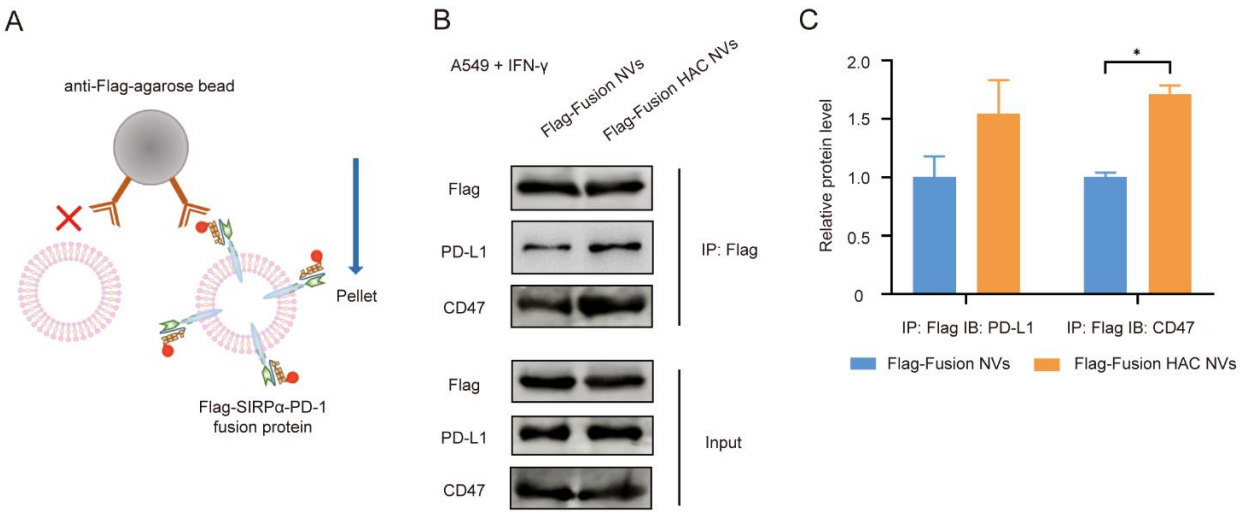

Figure S3. A) Schematic illustration for Flag antibody to pull down the Flag-SIRPα-PD-1 NVs. **B)** Representative western blot analysis of co-immunoprecipitation of Blank, Flag-Fusion, or Flag-Fusion HAC NVs interacting with PD-L1 and CD47 in A549. **C)** Statistics analysis of immunoprecipitation in (B) (n=3, **P*<0.05).

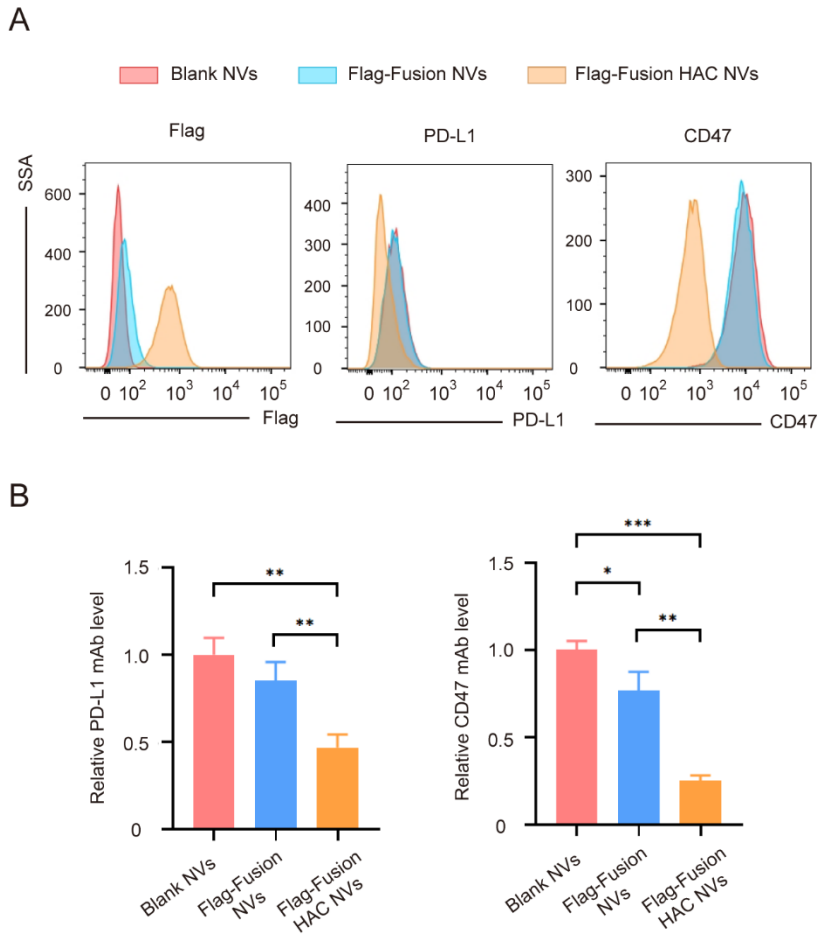

Figure S4. A) Binding and blocking efficiency of Blank, Flag-Fusion, or Flag-Fusion HAC NVs to PD-L1 and CD47 was measured by flow cytometry in A549. **B)** Statistics analysis of PD-L1 or CD47 mAb binding efficiency in (A) (n=3, **P*<0.05, ***P*< 0.01, and ****P*< 0.001).

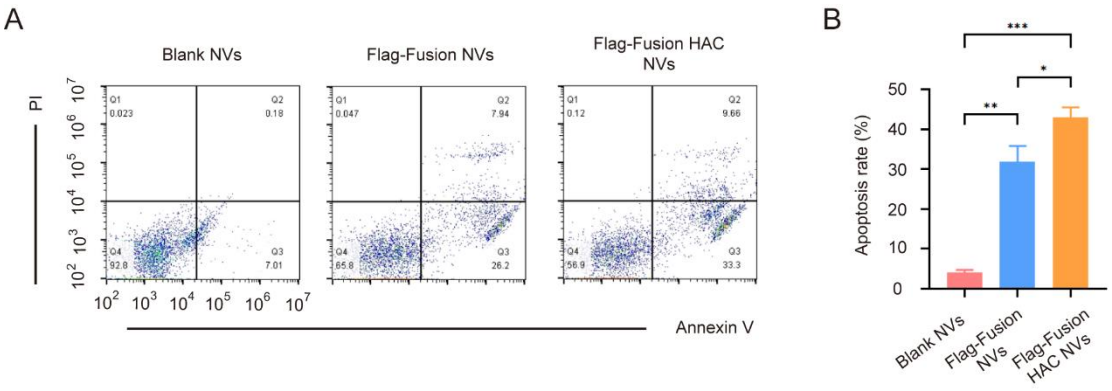

Figure S5. A) Apoptotic status of MDA-MB-231 cells treated with 100 μg Blank, Flag-Fusion, or Flag-Fusion HAC NVs for 24h. **B)** Statistics analysis of cells apoptosis in (A) (n=3, **P*<0.05, ***P*< 0.01, and ****P*< 0.001).

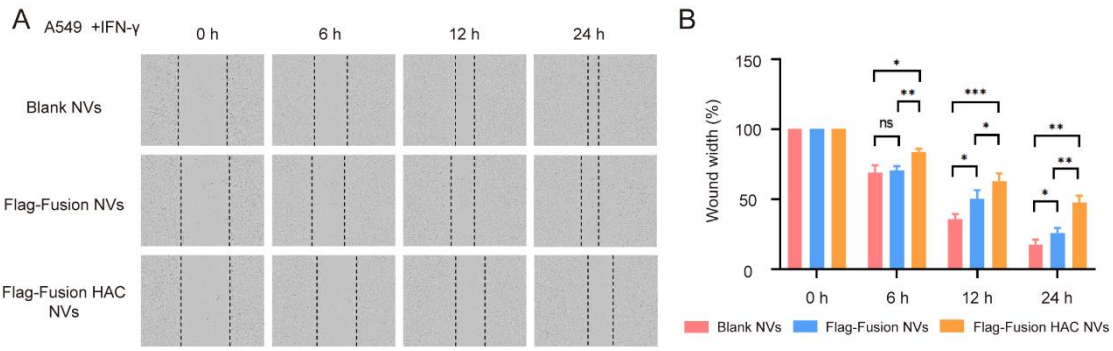

Figure S6. A) Wound healing assay of A549 cells treated with 100 μg Blank, Flag-Fusion, or Flag-Fusion HAC NVs, respectively. Migration was evaluated at 0, 6, 12 and 24 h time points after wounding, respectively. **B)** Statistics analysis of wound closure in (A) (n=3, **P*<0.05, ***P*< 0.01, and ****P*< 0.001).

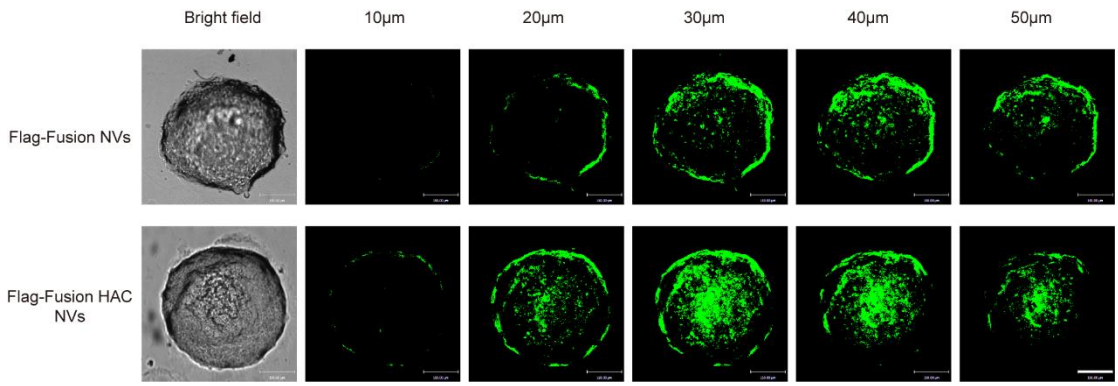

Figure S7. Penetration level of Flag-Fusion and Flag-Fusion HAC NVs in multicellular MDA-MB-231 tumor spheroids (Green: DiO-labeled NVs). Scale bar is 150 μm.

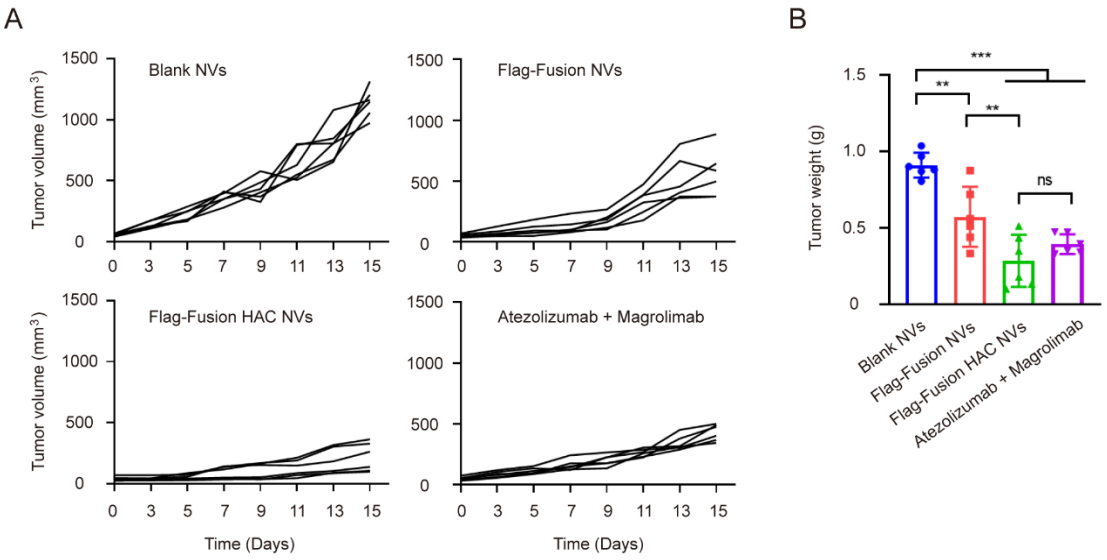

Figure S8. A) Change curve of individual tumor growth and **B)** Tumor weight treated with different treatments (n=6, ***P*< 0.01, ****P*< 0.001).

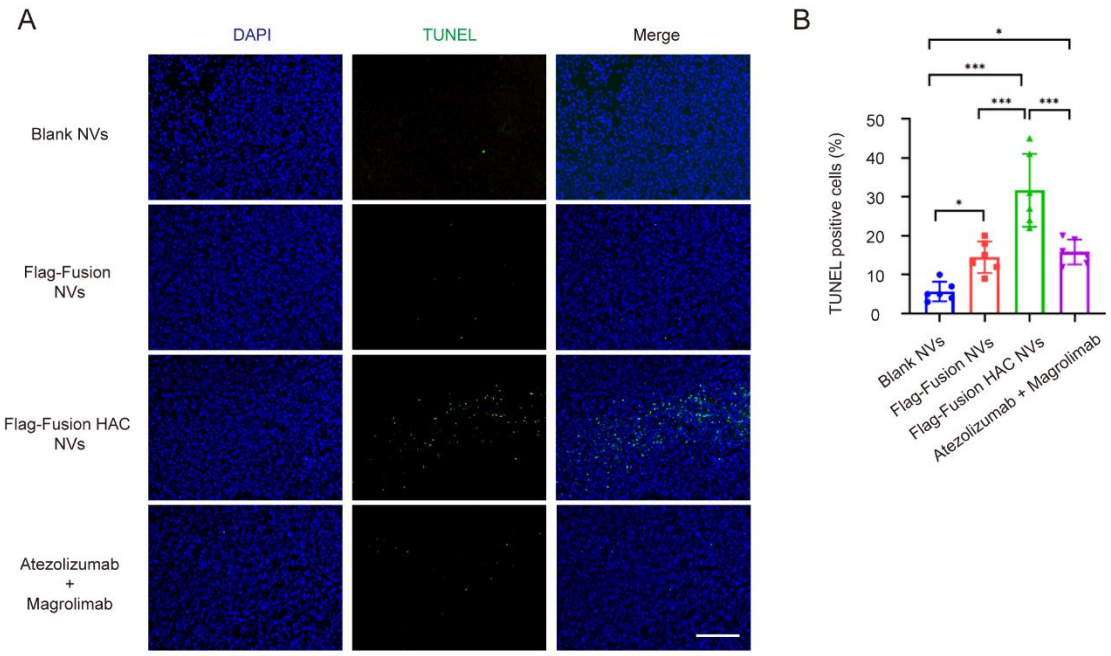

Figure S9. A) The fluorescent images of TUNEL staining of tumor tissues and **B)** Statistics analysis of TUNEL positive cells after different treatments (Blue: DAPI; Green: TUNEL staining; n=6, **P*<0.05, ****P*< 0.001). The bar scale is 100 μm.

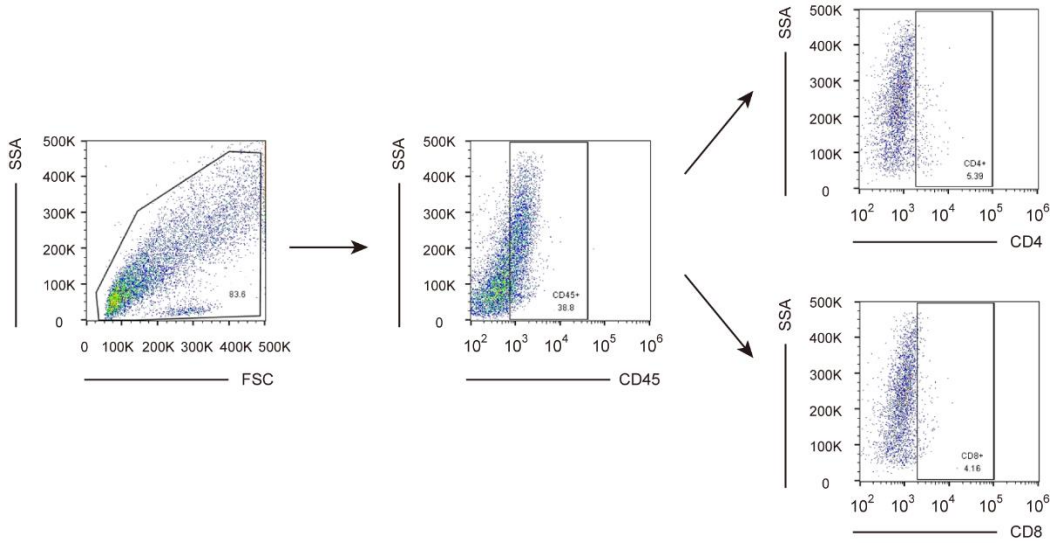

Figure S10. Flow cytometry gating strategy for analysis of the percentage of $CD45^+CD4^+$ and $CD45^+CD8^+$ T cells in tumor tissues.

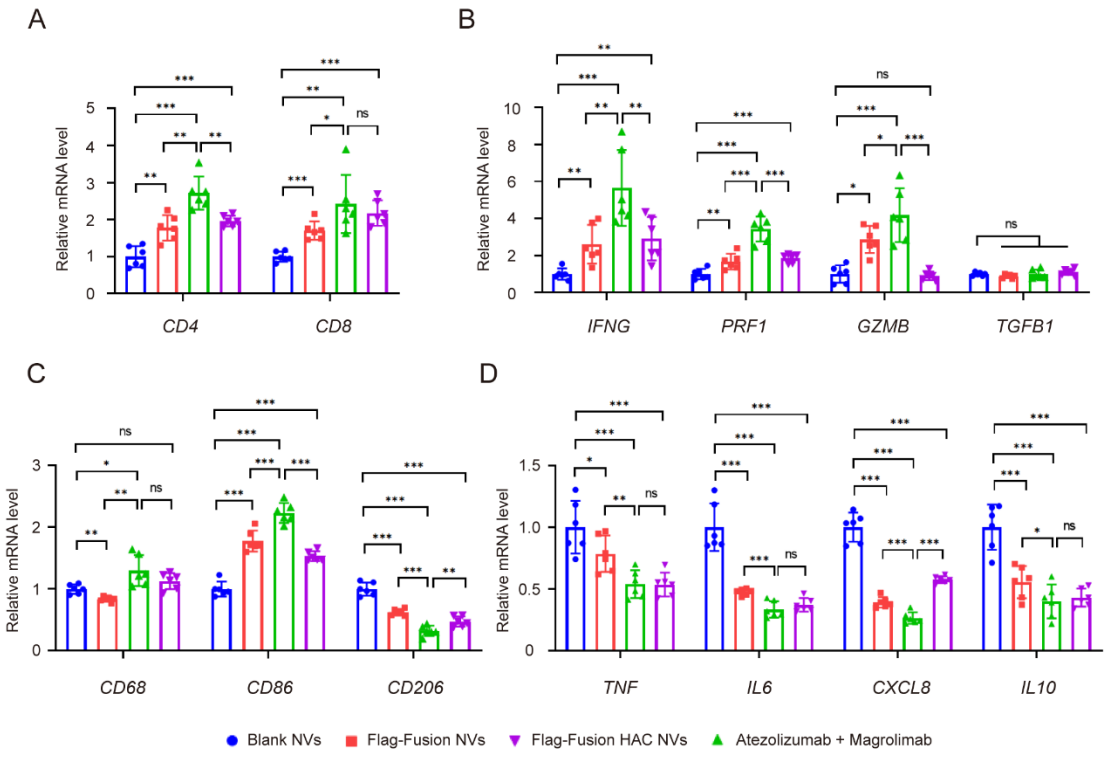

Figure S11. Statistics analysis of the mRNA expression of **A)** activated T lymphocyte markers, **B)** cytokines and chemokines produced by activated T lymphocyte, **C)** tumor-associated macrophage (TAM) markers and **D)** cytokines and chemokines produced by TAM were examined by RT-qPCR (n=6, **P*<0.05, ***P*< 0.01, and ****P*< 0.001).

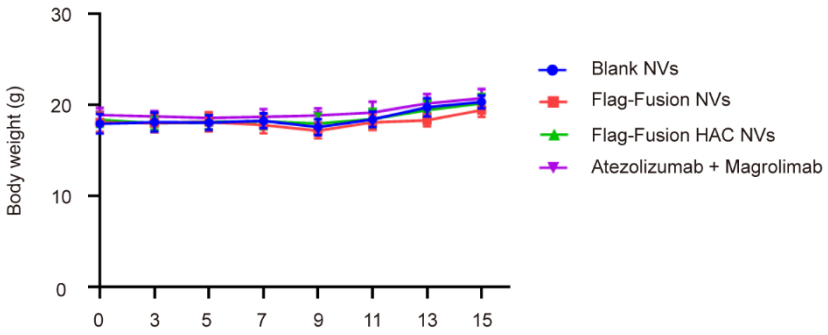

Figure S12. Body weight change of mice treated with different treatments (n=6).

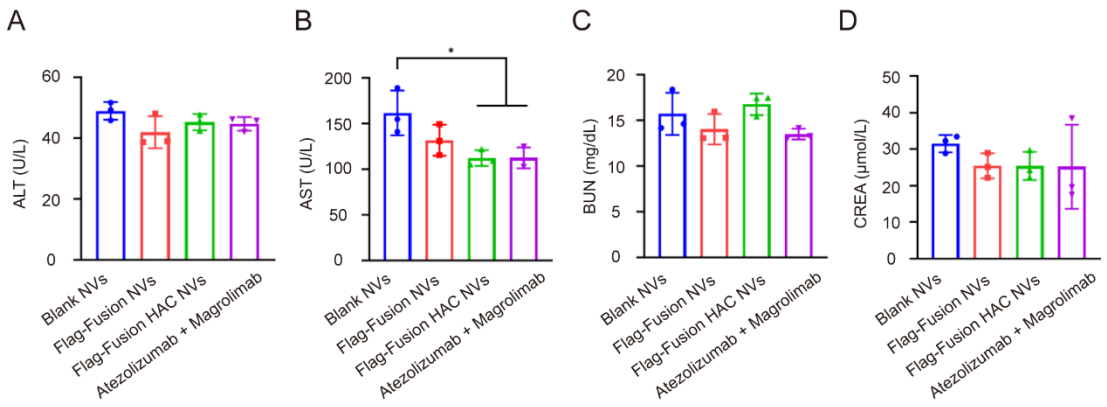

Figure S13. The biochemistry level of liver and renal function after different treatments. **A)** alanine transaminase (ALT), **B)** aspartate transaminase (AST), **C)** blood urea nitrogen (BUN) and **D)** creatinine (CRE) (n=3, **P*<0.05).

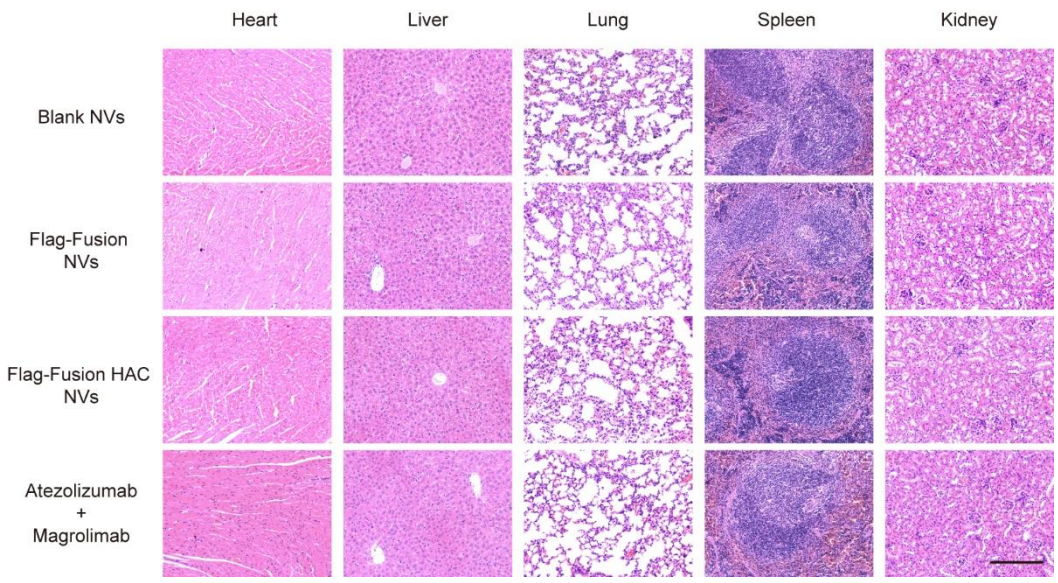

Figure S14. H&E staining of the main organs (heart, liver, lung, spleen and kidney) after different treatments. The bar scale is 100 μm.

A

Residue#	39	40	41	43	45	49	53	97	100	107
hPD-1	V	L	N	Y	M	N	K	L	A	A
hPD-1 HAC	H	V	I	H	E	G	T	V	V	I

B

Residue#	6	27	31	47	53	54	56	66	92
hSIRPα	V	V	I	E	K	E	H	S	V
hSIRPα HAC	I	I	F	V	R	Q	P	T	I

Table S1. The position of the mutated residues is denoted at the top of the table, and the high-affinity consensus (HAC) sequence (Red text) their corresponding sequence in wild-type (WT) allele (Black text) of PD-1 **A)** and SIRPα **B)** are showed in the table.

	Control	Blank NVs	Flag-Fusion NVs	Flag-Fusion HAC NVs	Atezolizumab + Magrolimab
RBC(M/μL)	10. 08±0. 68	8. 63±0. 3	8. 95±8. 2	8. 81±0. 33	9. 3±0. 37
HGB(g/dL)	14. 0±1. 29	12. 3±0. 45	12. 6±1. 21	12. 4±0. 42	13. 1±0. 45
PLT(K/μL)	817. 2±148. 34	1141. 2±269. 99	830. 8±282. 81	906. 3±260. 47	709+64. 97
WBC(K/μL)	6. 55±1. 06	6. 1±0. 67	5. 9±0. 68	4. 5±0. 88	4. 4±0. 94
HCT (%)	46. 8±4. 97	40. 5±1. 64	42. 6±4. 26	40. 1±1. 13	42. 6±1. 4
MCV (fL)	46. 4±2. 37	46. 7±1. 15	46. 3±1. 37	45. 5±0. 98	45. 8±0. 63
MCH (pg)	13. 9±0. 55	14. 4±0. 39	14. 0±0. 38	14. 1±0. 22	14. 1±0. 11
MCHC (g/L)	300. 0±5. 0	307. 8±10. 8	303. 3±6	308. 5±2. 7	308±3. 9
MPV (fL)	9. 43±0. 97	8. 95±0. 33	8. 95±0. 12	9. 0±0. 24	9. 5±0. 5

Table S2. Blood routine examination of mice treated with different treatments (n=6).